

Ultrasonic Spray Deposition of Metal Oxide Films on High Aspect Ratio  
Microstructures for 3D All-solid-state Li-ion Batteries

Peer-reviewed author version

VAN DEN HAM, Jonathan; GIELIS, Sven; VAN BAEL, Marlies & HARDY, An (2016)  
Ultrasonic Spray Deposition of Metal Oxide Films on High Aspect Ratio  
Microstructures for 3D All-solid-state Li-ion Batteries. In: ACS Energy Letters, 1, p. 1184-1188.

DOI: 10.1021/acsenergylett.6b00449

Handle: <http://hdl.handle.net/1942/22608>

# Ultrasonic Spray Deposition of Metal Oxide Films on High Aspect Ratio Microstructures for 3D All-Solid-State Li-ion Batteries

Evert Jonathan van den Ham<sup>‡</sup>, Sven Gielis<sup>‡</sup>, Marlies K. Van Bael and An Hardy\*

Hasselt University, Institute for Materials Research; Inorganic and Physical Chemistry and imec, division imomec, Martelarenlaan 42 3500 Hasselt, Belgium.

<sup>‡</sup>equal contribution

\*an.hardy@uhasselt.be

## Abstract

Deposition of functional materials on non-planar surfaces remains a challenge for various applications, among which 3D all-solid-state Li-ion batteries. In this letter we present a new process to deposit functional oxide materials on high aspect ratio microstructures, without the use of vacuum-based deposition methods. Using ultrasonic spray deposition in combination with metal citrate chemistry, we were able to deposit high quality coatings on Si micro-cylinders with an aspect ratio of 10. These results were achieved by controlling the precursor chemistry, wetting properties, gel mobility and precursor decomposition. The versatility of the process was shown by depositing titanium oxide (TiO<sub>2</sub>), lithium lanthanum titanate (Li<sub>0.35</sub>La<sub>0.55</sub>TiO<sub>3</sub>) and tungsten oxide (WO<sub>3</sub>) on Si micro-cylinders of 50 μm length, with an inter-cylinder distance of 5 μm. Finally, a proof of the 3D battery concept was achieved by coating of TiN / Si micro-cylinders with WO<sub>3</sub> using a minimized thermal budget to preserve the (oxidative) TiN current collector. This led to an almost threefold electrode capacity enhancement per footprint area, due to the high surface to bulk ratio of the 3D coating. Therefore, these results form a breakthrough in the field of solution-processing of non-planar microstructures. In addition, the flexibility, low-cost character and high up-scaling potential of this approach is very promising for various applications requiring coated 3D microstructures.

## Letter

The 3D integrated all-solid-state Li-ion thin film battery concept was first proposed by Notten and coworkers.<sup>1</sup> It combines all the benefits of an all-solid-state Li-ion battery but adds a significantly higher storage capacity by relying on high aspect ratio substrates. To date, all components for this battery concept have been achieved solely by means of vacuum deposition, either atomic layer deposition (ALD) or chemical vapor deposition (CVD): TiN current collectors, amorphous silicon or lithium titanate anodes, and a lithium phosphate electrolyte.<sup>2-7</sup> Though high quality films can be established with these methods, the vacuum conditions lead to significant disadvantages such as high cost and low throughput. In contrast, chemical solution deposition (CSD), is known as a low-cost deposition method yielding high quality planar films.<sup>8</sup> By combining liquid-based chemistry with various deposition methods such as spin-, spray- or dip-coating, high quality films can be established with high control over stoichiometry. Probably based on the wide use of spin-coating, the conviction that CSD is planarizing is often encountered. Nonetheless, previous studies using liquid misted deposition and spray-coating indicate that vacuum-free methods using solutions can be successful to coat non-planar surfaces.<sup>9,10</sup> However, limited aspect ratios were reached with these coating methods and parts of the substrates remained uncoated. Here, we report a breakthrough in this field, namely coating of non-planar surfaces with a high aspect - up to 10 - using CSD in combination with tailored chemistry and ultrasonic spray deposition.<sup>11</sup> Moreover, the method proposed here is generally applicable to a wide range of (multi)metal oxides, as demonstrated for TiO<sub>2</sub>, Li<sub>0.35</sub>La<sub>0.55</sub>TiO<sub>3</sub> (LLT) and WO<sub>3</sub>; all of interest to compile a 3D integrated all-solid-state Li-ion thin film battery.

In order to explain these unprecedented results, the tailoring of the physicochemical precursor properties as well as the specifics of the deposition method are held accountable. Aqueous citrate metal-ion solutions are selected as precursors, because they remain stable in ambient air and especially during ultrasonic spray deposition. These include, in the examples we present, titanium-,<sup>12</sup> lithium-, lanthanum- and tungsten-citrate complexes. To reduce the surface tension of these aqueous solutions, thereby enhancing their wetting on the substrate, they were mixed with ethanol. Since this may lead to citrate precipitation,<sup>13</sup> the ethanol to aqueous precursor volumetric ratio was set at 9:10, while maintaining low metal ion concentrations (10 to 50 mM). The tailored precursor was deposited on the 3D structured substrate by means of ultrasonic spray deposition; atomization of the precursor in combination with substrate heating leads to sufficiently small droplets that can penetrate between the high aspect ratio micro-cylinders, which are located only 5  $\mu$ m apart from each other. Equally important in achieving a continuous 3D film, is the choice of the deposition temperature during spraying, which is discussed further in more detail. In the end, fine tuning was possible by adjusting the nozzle distance and liquid flow rate. As a benchmarking material with multiple applications, this was first shown for TiO<sub>2</sub> by Gielis et al.<sup>11</sup> Besides the deposition of TiO<sub>2</sub> (Figure 1 a, b and c), the aqueous metal citrate precursor chemistry is in principle applicable to a wide range of metal ions.<sup>14</sup> Especially the deposition of multi-metal oxides is of interest, as excellent control over stoichiometry and homogeneous mixing can be achieved with these CSD precursors.<sup>8</sup> This is demonstrated by ultrasonic spray deposition of LLT solid-state electrolyte from an aqueous metal-citrate precursor solution (Figure 1 d, e and f).

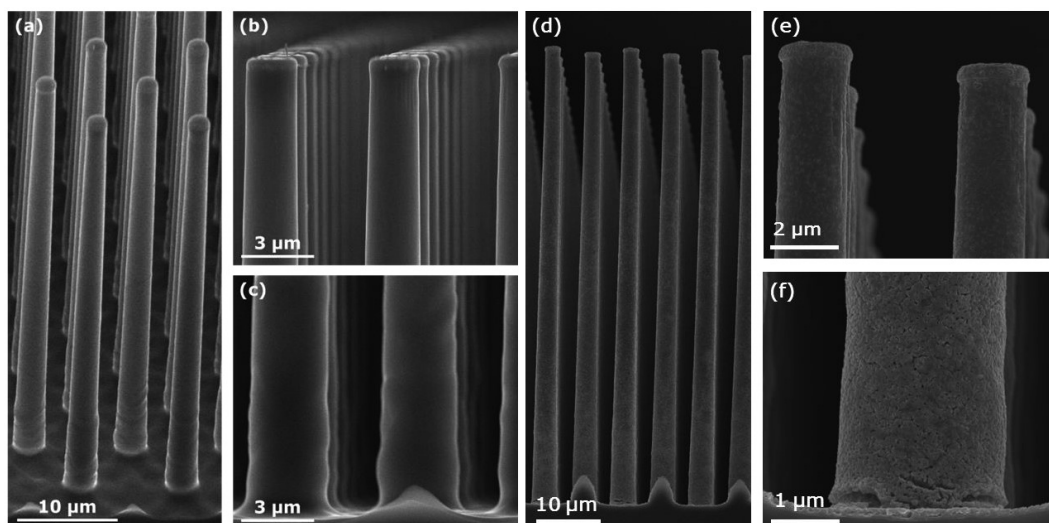


**Figure 1.** SEM micrograph of TiN / Si micro-cylinders, coated with (a), (b) and (c) the Ti-precursor (10 passes, 10 mM), annealed for 1 hour at 600°C in air; and (d), (e) and (f) with the Li-La-Ti-precursor (50 passes, 10 mM) submitted to a post-deposition anneal of 700°C for 4 hours in oxygen.

The temperature at which precursor droplets hit the surface of the substrate (i.e. the deposition temperature) proved to be the most important parameter to obtain a complete coating of the micro-cylinder. Due to a lack of gel immobilization at low deposition temperatures ( $<150^{\circ}\text{C}$ ) the precursor gel flows down the vertical structure,<sup>15</sup> yielding largely uncoated micro-cylinders and thick films at the bottom. In the other extreme, when the deposition temperature was increased to  $250^{\circ}\text{C}$ , the bottommost 5-6  $\mu\text{m}$  of the 50  $\mu\text{m}$  long micro-cylinders remained uncovered while clogging was observed higher up. This is probably due to high gel immobilization, caused by its decomposition, combined with strong thermophoretic forces at the bottom of the micro-cylinders.<sup>16</sup> Therefore no droplets are able to reach this part of the substrate at high deposition temperatures. The decomposition of the precursor, as analyzed by thermogravimetric analysis (TGA) shown in Figure 2, yields a clue to find the optimal deposition temperature. Empirically, the optimal deposition temperature of the Li-La-Ti-precursor was found at  $200^{\circ}\text{C}$ , which matches with the endothermic decomposition responsible for the first major weight loss of the heated precursor. The same correlation was found for  $\text{TiO}_2$  ( $180^{\circ}\text{C}$ ).<sup>12</sup>

A second important factor influencing the quality of the deposited coatings, is the precursor concentration. Lower precursor concentrations lead to smaller droplets hitting the heated substrate,<sup>16</sup> since significantly smaller amounts of non-evaporating material are available per droplet. These smaller droplets are quickly immobilized at the surface and prevent accumulation of the precursor gel down the micro-cylinders. Therefore, lower precursor concentrations of 10 or 25 mM, instead of 50 mM, resulted in more homogeneous layers.

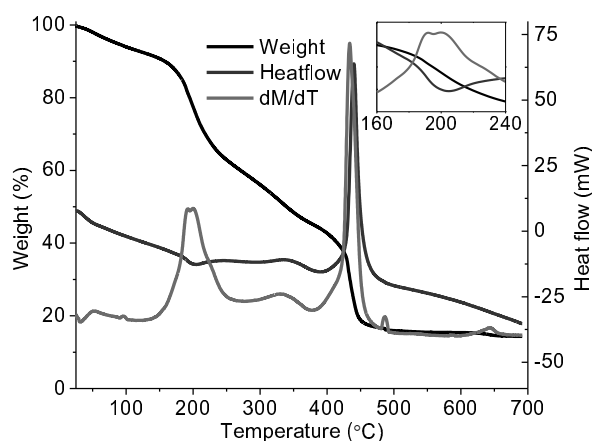


**Figure 2.** TGA-DSC analysis of the dried Li-La-Ti-precursor gel, measured in dry air with a heating rate of  $10^{\circ}\text{C}\cdot\text{min}^{-1}$ . Inset: enlargement of the 160-240°C (rescaled).

Although high quality coatings could be shown qualitatively by SEM micrographs (Figure 1), the thermal budget required to decompose the precursors and crystallize the  $\text{TiO}_2$  ( $600^{\circ}\text{C}$ )<sup>17</sup> as well as LLT ( $700^{\circ}\text{C}$ )<sup>18</sup> appeared to be too high to prevent the TiN current collector present on the micro-cylinders from oxidation, preventing successful functional measurements. This titanium oxynitride also hindered composition analysis of the  $\text{TiO}_2$  coatings. Hence, EDX and XRD were done on the LLT coatings, indicating the  $\text{Li}_{0.35}\text{La}_{0.55}\text{TiO}_3$  phase (JCPDS 46-465) is indeed formed (Figure 3).  $\text{TiO}_2$  (anatase and rutile, JCPDS 2-387 and 3-1122) and  $\text{La}_2\text{O}_3$  (JCPDS 1-83-1345) are also observed.

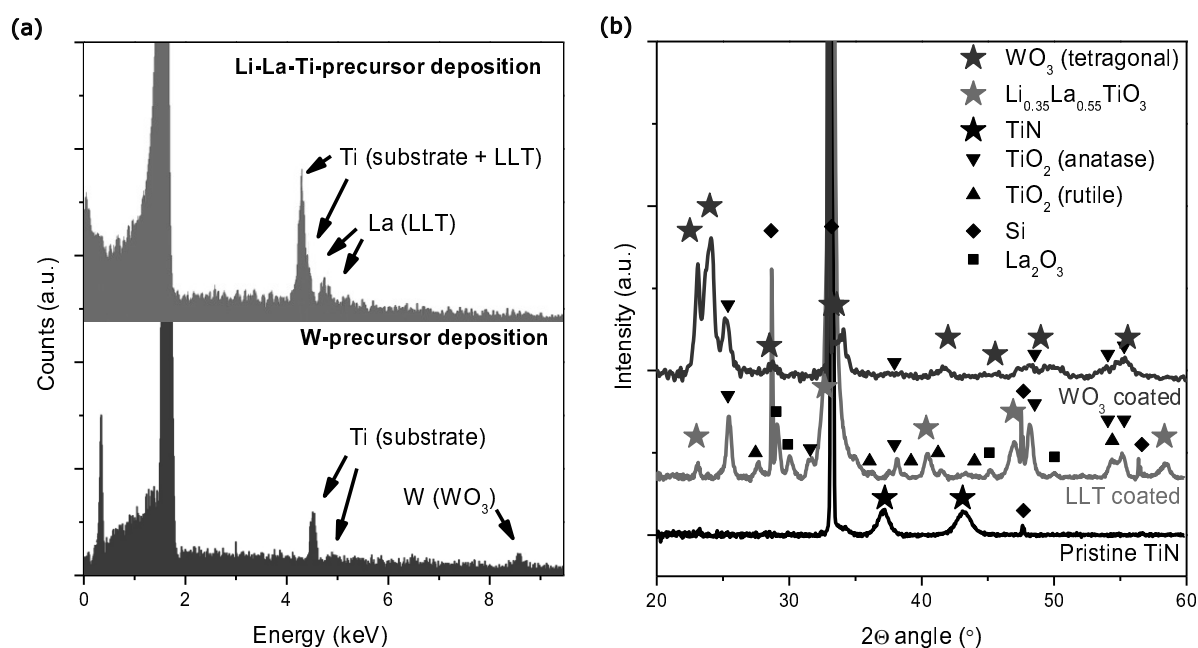


**Figure 3:** (a) EDX spectra and (b) X-ray diffractograms of TiN / Si micro-cylinders, coated with Li-La-Ti-precursor (50 passes, 10 mM) submitted to a post-deposition anneal of  $700^{\circ}\text{C}$  for 4 hours in oxygen and W-precursor (10 passes, 25 mM) subjected to a post-deposition anneal of  $600^{\circ}\text{C}$  for 1 hours in oxygen. EDX spectra were taken at the middle height of the pillars, whereas XRD probed a larger part of the micro-cylinder region of the samples.

The  $\text{TiO}_2$  phases arise due to oxidation of the TiN (JCPDS 1-87-626) current collector and it could segregate from LLT, together with  $\text{La}_2\text{O}_3$  formation, as the result of the relative long anneal (4 hours) leading to lithium diffusion into the oxidized TiN/ $\text{TiO}_2$  underneath and / or doping of Li into  $\text{TiO}_2$ . In addition, sharp Si (JCPDS 1-80-18) reflections are observed as a result of broken Si-micro-cylinders due to sample handling. Full compositional analysis by EDX was not possible, since Li is undetectable by EDX, and Ti-signals are interfered by the titanium(oxy)nitride already present underneath the LLT coating.

In order to study the functional properties of 3D coatings achieved by the approach presented in this study,  $\text{WO}_3$  was used because it is reported to crystallize at low temperatures ( $300^\circ\text{C}$ ).<sup>19</sup> As a negative electrode,  $\text{WO}_3$  has a high volumetric capacity ( $640 \text{ mAh}\cdot\text{cm}^{-3}$ ).<sup>20</sup> In addition, the relatively high intercalation voltage of  $\text{WO}_3$  (2.7 and 2.4 V vs.  $\text{Li}^+/\text{Li}$ ) ensures that only the capacity of the  $\text{WO}_3$  is probed during galvanostatic measurements, instead of the  $\text{TiO}_2$  (lithiation at 1.7 V vs.  $\text{Li}^+/\text{Li}$ )<sup>20</sup> that tends to be formed by oxidation of the TiN current collector. Similar to the process described above, the deposition of  $\text{WO}_3$  was optimized to coat the micro-cylinders, yielding tetragonal  $\text{WO}_3$  (JCPDS 1-85-807) in the coatings annealed for 1 hour at  $600^\circ\text{C}$  (Figure 3), in addition to  $\text{TiO}_2$  (anatase) as a result of TiN oxidation. For functional measurements, the thermal anneal was therefore restricted to an absolute minimum (10 minutes at  $500^\circ\text{C}$ ) to decompose the deposited W-precursor with residual organics and form the oxide material. This yields partially crystallized, electrochemically active  $\text{WO}_3$  coatings as illustrated with the galvanostatic measurements showing (de)lithiation of the  $\text{WO}_3$  films (Figure 4).

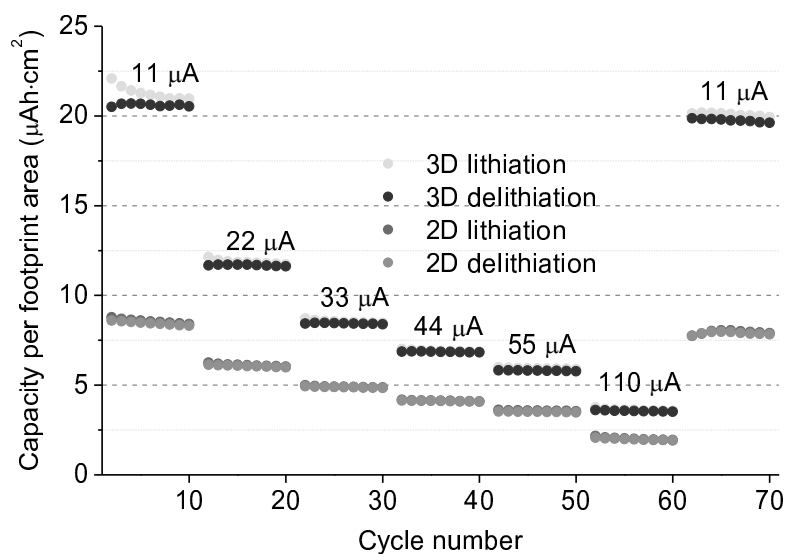


**Figure 4.** 3D  $\text{WO}_3$  coated micro-cylinders compared to a planar (2D) sample; both prepared with W-precursor deposited at  $180^\circ\text{C}$  (10 cycles with 25 mM) with a post deposition anneal of 10 minutes at  $500^\circ\text{C}$  in static air. Galvanostatic measurements were done at various currents between 1.75 and 4.0 volts (vs.  $\text{Li}^+/\text{Li}$ ) in 1.0 M  $\text{LiClO}_4$  in PC.

To compare planar (2D) and 3D depositions, the same amount of material was deposited on planar and 3D TiN coated substrates (10 passes, 25 mM). Hence, planar (2D) films with a thickness of 240 nm perform differently due to longer diffusion lengths, compared to the thinner 3D structured samples consisting of 30 nm thick  $\text{WO}_3$  films (with an 8 fold larger current collector surface area, but consisting of the same  $\text{WO}_3$  volume). The same current density per footprint area should result in a larger capacity for the thinner, 3D structured,

WO<sub>3</sub> films because the current density per coating area is significantly lower than for the 2D sample. Figure 4 shows that is indeed the case: 3D structured films exhibit a near threefold capacity increase compared to 2D films. Although several issues are still to be overcome – especially with respect to the thermal stability of the current collector – the deposition of WO<sub>3</sub> as a proof-of-principle shows a huge potential for realizing the 3D battery concept established with ultrasonic spray deposition.

In conclusion, we showed that an optimized precursor and fine-tuned ultrasonic spray deposition yields a complete metal-oxide coating on micro-cylinders with an aspect ratio of 10 and an inter-cylinder distance of 5 μm. Achieving these results via chemical solution deposition forms a major breakthrough, as a cost reduction and possibilities towards upscaling are enabled. Since several (multi-)metal oxides can be deposited, serving as electrode and solid electrolyte materials, this process offers a high degree of flexibility to achieve a 3D integrated all-solid-state Li-ion battery. The near threefold capacity increase, demonstrated for the 3D structured WO<sub>3</sub> electrode compared to a planar counterpart, illustrates that the morphology of the materials can be controlled with this method. As the aqueous metal-citrate precursor solutions have been developed for a very broad range of metal-ions,<sup>12,21</sup> this breakthrough can have a huge impact in different fields of application. This process is especially of interest where low cost and high throughput fabrication of (multi)metal-oxide coatings are needed to achieve large surface areas per footprint area, combined with a high degree of structure.

## Experimental

Mono-metal aqueous citrate solutions were prepared for Li<sup>+</sup>, La<sup>3+</sup>, Ti<sup>4+</sup> and W<sup>6+</sup>. The Li-citrate was prepared by dissolution of lithium citrate (99%, Sigma Aldrich) in water, while stirring at room temperature. La-citrate and Ti-citrate were prepared as stated previously by Hardy et al.<sup>22</sup> W-citrate was prepared by mixing tungstic acid (99,9%, Sigma Aldrich) and citric acid (99,9%, Sigma Aldrich) under reflux conditions for 24 hours, with a 4:1 citrate to tungsten ratio. Next, the pH was raised to 12 with NH<sub>3</sub> (32%, Merck), and left to stir for 24 hours again, yielding a final pH of 8. The aqueous mono-metal ion precursor solutions were filtered using a membrane filter (Nalgene, 0.2 μm) to remove particles, such as dust, impurities and undissolved fractions. Subsequently, their exact concentrations were determined by ICP-AES (Optima 3000, PerkinElmer). Mixing of the mono-metal aqueous solutions was based on the desired stoichiometry of the LLT oxide, although 10% excess of Li was applied to compensate for Li-loss. Finally, ethanol (absolute, VWR) was added to yield a 9:10 ethanol to water ratio for all precursors, with a total metal ion concentration of 10 to 50 mM. The precursors were deposited separately on substrates consisting of micro-cylinders prepared by reactive ion etching and consequently coated with TiN using chemical vapor deposition (imec, Heverlee, Belgium). These micro-cylinders were 50 μm long, were separated by 5 μm of inter-cylinder distance and had a radius of 1.0 (top) to 1.5 (bottom) μm. As a planar (2D) comparison, TiN coated Si substrates were used (imec, Heverlee, Belgium). The substrates were treated by UV/O<sub>3</sub> (60°C, 30 min., Novascan PSD Pro Series) prior to the deposition. The precursors were deposited onto the substrates via ultrasonic spray deposition (Exacta Coat, Sono-Tek cooperation) using the Accumist nozzle (Sono-Tek cooperation). The deposition temperature was set at various values between 150 and 250 °C. The precursors were dispensed at 0.2 ml·min<sup>-1</sup> and the N<sub>2</sub> carrier gas pressure was set at 1.5 psi. The spray nozzle was located 2.6 cm above the substrate and moved with a speed of 100 mm·s<sup>-1</sup>. The spray cycle was repeated 10 to 50 times with a waiting time of 5 seconds. After deposition, a sequential hot plate treatment, in static air, was carried out at 180, 300 and 600°C (2 min.). Finally, a post-deposition anneal was applied. For the Ti-precursor (10 mM) coated samples, 1 hour at 600°C in static air was applied. In case of Li-La-Ti-precursor (10 mM total metal ion concentration) coated samples, a post deposition

anneal of 4 hours at 700°C in oxygen (0.5 ml·min<sup>-1</sup>) was used in a tube furnace with a heating rate of 10 °C·min<sup>-1</sup>. The W-precursor (25 mM) coated samples were annealed 10 minutes at 500°C or 1 hour at 600°C, both in static air. The obtained films were stored in under Ar atmosphere. The thermal decomposition profile of the Li-La-Ti-precursor gel, obtained by drying the precursor solution at 60°C overnight, was investigated by thermogravimetric analysis with coupled differential scanning calorimetry (TGA-DSC, TA instruments SDT Q600). 6 mg of the powder was heated ramped at 10°C·min<sup>-1</sup> up to 700°C using dry air (0.1 L·min<sup>-1</sup>) in an alumina crucible. The deposited films were evaluated by means of scanning electron microscopy (SEM, FEI NOVA 200) and energy dispersive X-ray analysis (SEM with EDX, FEI Quanta 200F). Galvanostatic measurements were done with an Autolab PGSTAT128N (Metrohm, Utrecht, the Netherlands), using a three electrode setup in combination with a custom made Teflon cell filled with 1.0 M LiClO<sub>4</sub> dissolved in polycarbonate (Soulbrain MA, USA). The sample was used as the working electrode, metallic lithium (99,9% Sigma Aldrich) served as the counter and reference electrodes. During the galvanostatic measurements, the test cell was operated at 20.0 °C via a custom made temperature control chamber in an argon filled glovebox.

## Acknowledgements

The authors acknowledge imec (Heverlee, Belgium) for providing substrates and SEM measurements during this project. K. Elen (XRD), G. Bonneux (EDX) and W. Marchal (TGA) are acknowledged for contribution to this study. BOF IOF UHasselt is acknowledged for financial support.

## References

- (1) Notten, P. H. L.; Roozeboom, F.; Niessen, R. A. H.; Baggetto, L. 3-D Integrated All-Solid-State Rechargeable Batteries. *Adv. Mater.* **2007**, 19, 4564–4567.
- (2) Baggetto, L.; Knoops, H. C. M.; Niessen, R. a. H.; Kessels, W. M. M.; Notten, P. H. L. 3D Negative Electrode Stacks for Integrated All-Solid-State Lithium-Ion *Microbatteries*. *J. Mater. Chem.* **2010**, 20, 3703.
- (3) Xie, J.; Harks, P.-P. R. M. L.; Li, D.; Raijmakers, L. H. J.; Notten, P. H. L. Planar and 3D Deposition of Li<sub>4</sub>Ti<sub>5</sub>O<sub>12</sub> Thin Film Electrodes by MOCVD. *Solid State Ionics* **2016**, 287, 83–88.
- (4) Xie, J.; Oudenhoven, J. F. M.; Harks, P.-P. R. M. L.; Li, D.; Notten, P. H. L. Chemical Vapor Deposition of Lithium Phosphate Thin-Films for 3D All-Solid-State Li-Ion Batteries. *J. Electrochem. Soc.* **2014**, 162, A249–A254.
- (5) Donders, M. E.; Oudenhoven, J. F. M.; Baggetto, L.; Knoops, H. C. M.; van de Sanden, M. C. M.; Kessels, W. M. M.; Notten, P. H. L. All-Solid-State Batteries: A Challenging Route Towards 3D Integration *ECS Trans.* **2010**, 33, 213–222.
- (6) Eustache, E.; Tilmant, P.; Morgenroth, L.; Roussel, P.; Rolland, N.; Brousse, T.; Lethien, C. High Surface Capacity Li-Ion All Solid State 3D Microbattery Based On Anatase TiO<sub>2</sub> Deposited By ALD On Silicon Microstructures. *ECS Trans.* **2013**, 58, 119–129.
- (7) Baggetto, L.; Oudenhoven, J. F. M.; Van Dongen, T.; Klootwijk, J. H.; Mulder, M.; Niessen, R. A. H.; De Croon, M.; Notten, P. H. L. On the Electrochemistry of an Anode Stack for All-Solid-State 3D-Integrated Batteries. *J. Power Sources* **2009**, 189, 402–410.
- (8) Schwartz, R.; Schneller, T.; Waser, R. Chemical Solution Deposition of Electronic Oxide Films. *Comptes Rendus Chim.* **2004**, 7, 433–461.



- (9) Lunt, M. Liquid Source Misted Chemical Deposition (LSMCD) - A Critical Review. *Integr. Ferroelectr.* **1995**, 10, 39–53.
- (10) Shaijumon, M. M.; Perre, E.; Daffos, B.; Taberna, P.-L.; Tarascon, J.-M.; Simon, P. Nanoarchitected 3D Cathodes for Li-Ion Microbatteries. *Adv. Mater.* **2010**, 22, 4978–4981.
- (11) Gielis, S.; Hardy, A.; Van Bael, M. K. Conformal Coating on Three-Dimensional Substrates. EP 2 947 178 A1, **2015**.
- (12) Truijen, I.; Van Bael, M. K.; Rul, H. Van Den; D’Haen, J.; Mullens, J. Synthesis of Thin Dense Titania Films via an Aqueous Solution-Gel Method. *J. Sol-Gel Sci. Technol.* **2006**, 41, 43–48.
- (13) Dengel, A. C.; Griffith, W. P.; Powell, R. D.; Skapski, A. C. Studies on Transition-Metal Peroxo Complexes. Part 7. Molybdenum(VI) and Tungsten(VI) Carboxylato Peroxo Complexes, and the X-Ray Crystal Structure of  $K_2[Mo(O_2)_2(glyc)] \cdot 2H_2O$ . *Dalt. Trans.* **1987**, 991–995.
- (14) Van Bael, M. K.; Nelis, D.; Hardy, A.; Mondelaers, D.; Van Werde, K.; D’Haen, J.; Vanhoyland, G.; Van den Rul, H.; Mullens, J.; Van Poucke, L. C.; Frederix, F.; Wouters, D. J. Aqueous Chemical Solution Deposition of Ferroelectric Thin Films. *Integr. Ferroelectr.* **2002**, 45, 113–122.
- (15) Van Bael, M. K.; Hardy, A.; Mullens, J. Aqueous Precursor Systems. *Chemical solution deposition Of functional oxide thin films*; Springer-Verlag Wien, 2013; pp 93–140.
- (16) Perednis, D.; Gauckler, L. J. Thin Film Deposition Using Spray Pyrolysis. *J. Electroceramics* **2005**, 14, 103–111.
- (17) Truijen, I.; Hardy, a.; Van Bael, M. K.; Van den Rul, H.; Mullens, J. Study of the Decomposition of Aqueous Citratoperoxo-Ti(IV)-Gel Precursors for Titania by Means of TGA-MS and FTIR. *Thermochim. Acta* **2007**, 456, 38–47.
- (18) Van den Ham, E. J.; Peys, N.; De Dobbelaere, C.; D’Haen, J.; Mattelaer, F.; Detavernier, C.; Notten, P. H. L.; Hardy, A.; Van Bael, M. K. Amorphous and Perovskite  $Li_{3x}La_{(2/3)-x}TiO_3$  (thin) Films via Chemical Solution Deposition: Solid Electrolytes for All-Solid-State Li-Ion Batteries. *J. Sol-Gel Sci. Technol.* **2015**, 73, 536–543.
- (19) Nishio, K.; Tsuchiya, T. Electrochromic Thin Films Prepared by Sol-Gel Process. *Sol. Energy Mater. Sol. Cells* **2001**, 68, 279–293.
- (20) Van den Ham, E. J.; Elen, K.; Kokal, I.; Yagci, M. B.; Peys, N.; Bonneux, G.; Ulu, F.; Marchal, W.; Van Bael, M.; Hardy, A. From Liquid to Thin Film: Colloidal Suspensions for Tungsten Oxide as an Electrode Material for Li-Ion Batteries. *RSC Adv.* **2016**, 6, 51747–51756.
- (21) Peys, N.; Ling, Y.; Dewulf, D.; Gielis, S.; De Dobbelaere, C.; Cuypers, D.; Adriaensens, P.; Van Doorslaer, S.; De Gendt, S.; Hardy, A.; Van Bael, M. K.  $V_6O_{13}$  Films by Control of the Oxidation State from Aqueous Precursor to Crystalline Phase. *Dalton Trans.* **2013**, 42, 959–968.
- (22) Hardy, A.; Mondelaers, D.; Van Bael, M. K.; Mullens, J.; Van Poucke, L. C.; Vanhoyland, G.; D’Haen, J. Synthesis of  $(Bi,La)_4Ti_3O_{12}$  by a New Aqueous Solution-Gel Route. *J. Eur. Ceram. Soc.* **2004**, 24, 905–909.